

Direct Numerical Simulation of Turbulent Flows in a Subchannel of Tight Lattice Fuel Pin Bundles of Nuclear Reactors

Project Representative

Hisashi Ninokata Tokyo Institute of Technology

Authors

Hisashi Ninokata^{*1}, Norio Atake^{*1}, Emilio Baglietto^{*1},

Takeharu Misawa^{*2} and Takuma Kano^{*2}

*1 Tokyo Institute of Technology

*2 Japan Atomic Energy Research Institute

The direct numerical simulation has been applied to a fully-developed single-phase turbulent flow analysis for triangular pin bundles of infinite array configuration. The DNS algorithm adopted here is based on the finite difference method being extended to the boundary-fitted coordinate system, verified for a number of numerical benchmarks and turbulent flows in flow channels of simple geometry, and can concentrate grids efficiently near the distorted wall boundary such as fuel pin bundle configurations. A comparison between calculation and experiment has been made for the experimental data but limited to a turbulent flow of the friction Reynolds number $Re_\tau = 1,400$, the lowest available, inside a bundle with the pitch-to-diameter ratio (P/D) equal to 1.2. Then calculations have been carried out for bundles of $P/D=1.2$, 1.1 and 1.05 with different Reynolds numbers to investigate the influences of the subchannel pin wall and the gap sizes on the turbulence characteristics and on the distributions of mean axial velocity, secondary flow and wall shear stress.

Keywords: turbulent flow, anisotropy, DNS, rod bundle, secondary flow

1. INTRODUCTION

Liquid-metal-cooled fast reactors (LMFR) that are aimed at attaining high fuel burn-up and fuel breeding adopt the triangular fuel pin array configuration with the tight lattice pitch in order to increase the fuel-to-moderator ratio, thus to enhance the fuel utilization and extend the core life. In these options, it is necessary to evaluate the cladding temperature distribution and to identify the hot spot with high accuracy.

In the past, the direct numerical simulation (DNS) has been hardly applied to the turbulent flows inside a fuel pin bundle because of the computing power available to date. Therefore numerical estimation of detailed thermal hydraulics fields in pin bundles has been mainly carried out by the RANS (Reynolds Averaged Navier-Stokes model) approach ([1], [2], [3]). In general, however, it is often the case for the RANS turbulence models to fail in predicting secondary flows of the second kind, which is caused by the turbulence anisotropy and is supposed to have an important influence on the velocity and temperature profiles of the coolant in complex flow channel geometry. Furthermore the use of the wall function model substantially limits its applicability to these flows. The present authors noted the desir-

ability of applying DNS using the finite difference method, extended to the boundary-fitted coordinate system. To make the DNS more practical we have eluded the difficulty with the compromise of renouncing calculation of the higher-order moments, e.g., skewness, flatness, etc., that swell the number of grids required for ensuring accuracy. Thus, we limit our estimations to the averaged velocity profile, second-order moments of turbulence, i.e., turbulence intensity, and Reynolds shear stress for deriving which we utilize the minimum number of grids necessary for ensuring requisite accuracy. In this work, this form of direct numerical simulation using finite difference method, extended to boundary fitted coordinate system, is applied to turbulent flow over triangular array pin bundle. Calculation results are compared with experiments in order to verify that the method simulates turbulent fields accurately. Moreover, reliable results for turbulent flows of various Reynolds numbers and pitch to diameter ratios are provided by the present simulations.

2. COMPUTATIONAL PROCEDURE

2.1. Basic Equations and Computational Method

The governing Navier-Stokes equations, extended to the

boundary-fitted coordinate system [4] are the mass and the momentum conservation equations and a mean axial pressure gradient is an input that drives incompressible flows through the pin bundles. The numerical method is based on the fractional step method, with the collocated grid system. For the spatial derivatives, the second order accurate scheme is applied to the convection terms. The second order accurate central difference scheme for other terms while near the wall the viscous term is interpolated using inner three points. An explicit Adams-Bashforth scheme is used for the time-advancement of convection and diffusion terms. The Poisson-type pressure equation is solved by the scaling conjugate gradient method using FFT in the axial direction. The contravariant velocity components are transformed from the Cartesian velocity components by 4-point interpolation.

2.2. Computational Domain and Boundary Condition

DNS calculations in this work are limited to infinite array pin bundles. A fraction of the triangular infinite array bare pin bundle is shown in Fig. 1. This pin bundle can be divided into minimum unit cells taking advantage of a maximum symmetry of a subchannel of the infinite array pin bundle. In this case one minimum unit cell is 1/6 of the subchannel. The computational domains consist of the combination of minimum unit cells with appropriate periodic boundary conditions. Namely, the non-slip condition is imposed on the fuel wall surface, and a periodic condition is imposed at the flow inlet and outlet with the axial spacing of $3.2 \times D_h$. Figure 1 also shows the computational domain that consists of 12 minimum unit cells, in which the periodic condition is applied to the boundary surfaces that face each other across the fuel pin. A combination of the computational domains

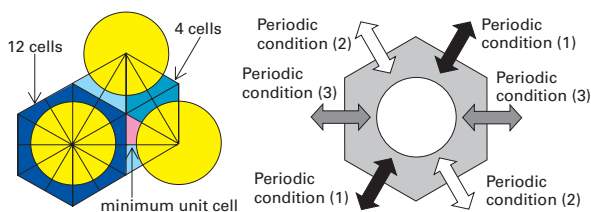


Fig. 1. Computational domain and boundary condition

of 12 cells can compose an infinite array pin bundle consistently.

3. RESULTS

3.1. Computational Cases

Simulations of the flows of friction Reynolds number $Re_\tau = 400$ and 600 have been carried out for the pitch-to-diameter ratio $P/D = 1.2, 1.1$ and 1.05 , and the flows of $Re_\tau = 1000$ and 1400 for $P/D = 1.2$. See Table 1 with computational conditions where Case D is compared to the experiment by Trupp, et al. [5] having the bulk Reynolds number of 23,760. This experimental result corresponds to the lowest bulk Reynolds number data in a triangular pin bundle and is one of the few in open literature in which details of turbulent characteristics are available.

The fully-developed turbulent flow is identified by the fact that the sample data of the averaged turbulent energy, bulk velocity, and wall shear stress show statistically a steady-state. The instantaneous velocities obtained by the present simulation are time-averaged and space-averaged in the axial direction. Those are also ensemble-averaged over all minimum unit cells, and are described using cylindrical coordinate system.

3.2. Comparison of the Velocity Profile with Wall Function Model

Figure 2 shows a comparison of the axial flow velocity profile for $P/D=1.05$ with $Re_\tau = 600$ (Case B3) with that given by a popular wall function model used in RANS. It has been revealed that in the cases of $P/D = 1.1$ and $P/D = 1.05$, difference of axial velocity distribution between center region and gap region extends. It corresponds to the increase in flow area of the center region (toward $\phi = 30^\circ$) and the decrease in gap region (toward $\phi = 0^\circ$) as P/D decreases. This is an example that illustrates a limitation of the use of the wall-function model in the RANS approach to the tight lattice bundle calculations in relatively low Reynolds number turbulent flow regime. It is noted here that, however for more open lattice bundles with $P/D > 1.2$, the velocity profiles for $\phi = 0^\circ \sim 30^\circ$ overlap with that given by the wall function model.

Table 1 Calculation conditions of the simulation cases

Case	Re_τ	P/D	$N_\phi \times N_r \times N_z$	$r^+ \Delta\phi$	Δr^+	Δz^+	Δt^+	Bulk Re_b
A1	400	1.2	384×28×128	6.2~7.3	1.0~12.8	10.0	1.5E-4	5,972
A2		1.1	624×34×128	6.1~7.3	1.0~12.8	10.0	1.5E-4	5,969
A3		1.05	864×41×128	6.5~7.8	1.0~12.8	10.0	1.5E-4	5,863
B1	600	1.2	576×40×160	6.2~7.3	1.0~13.7	12.0	1.5E-4	9,181
B2		1.1	864×50×160	6.6~7.9	1.0~13.4	12.0	1.5E-4	9,384
B3		1.05	1152×60×160	7.4~8.8	1.0~13.5	12.0	8.0E-5	9,646
C	1,000	1.2	912×67×256	6.5~7.7	1.0~16.8	14.0	1.5E-4	16,276
D	1,400	1.2	1056×80×320	7.9~9.3	1.0~16.9	14.0	1.2E-4	23,763

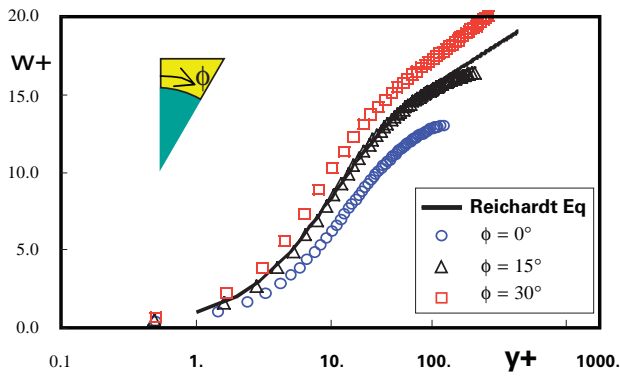


Fig. 2 Comparisons of axial velocity profile at $\phi = 0^\circ, 15^\circ$ and 30° ($P/D=1.05, Re_\tau = 600$)

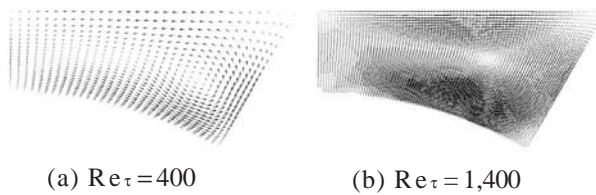


Fig. 3 Secondary flow distributions ($P/D = 1.2$)

3.3. Influence of Reynolds Number on Turbulent Flow Fields

DNS calculations for the lower bulk Re numbers with $P/D = 1.2$ have shown that the distribution shape of Reynolds normal and shear stresses varies from the open to gap region, i.e., from $\phi = 30^\circ$ to 0° while, for the higher Re number ($> 20,000$) flows, its dependency on the location is found weak. This DNS result is considered to have resulted from the variance of turbulent boundary layer with increasing Reynolds number. The range of bulk Reynolds number from 4,000 to 24,000 is considered within the transition region from laminar flow to turbulent flow. In this range of Reynolds number, thickness of turbulent boundary layer varies on a large scale, because the turbulent flow in this range of Reynolds number has strong viscosity near the wall in comparison with turbulent flow of $Re_{bulk} > 24,000$. Without solid experimental evidences, however, it is our inference that, for flows in pin bundles, the localized turbulent-laminar transition is taking place with the lower Re_{bulk} than $\sim 20,000$ and this Reynolds number would change as P/D changes. Further phenomenological and computational studies are on-going efforts for the confirmation.

For example, as the bulk Reynolds number increases from 6,000 to 24,000, a peak location of the wall shear stress moves from $\phi = 25^\circ$ (Cases A1, B1) to 20° (Case D), and the distribution becomes flatter. In fact it has been shown experimentally by Trupp et al. [5] that in much higher Re_{bulk} region, the wall shear stress distributions were shown to hardly vary. DNS results are in agreement with this trend.

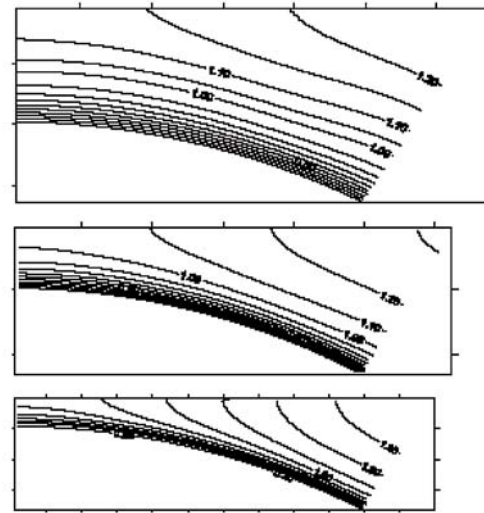


Fig. 4 Axial velocity profile ($Re_\tau = 400, P/D = 1.2, 1.1, \text{ and } 1.05$)

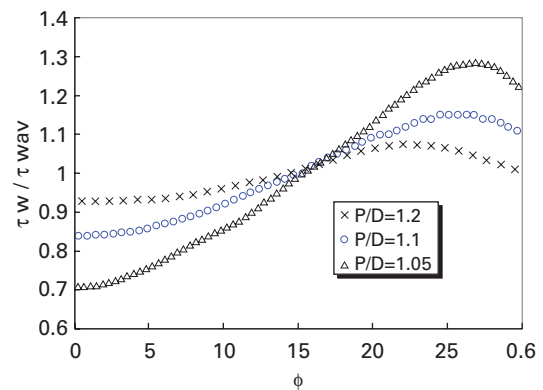


Fig. 5 Wall shear stress distributions ($Re_\tau = 400, P/D = 1.2, 1.1, \text{ and } 1.05$)

Also they indicate that the flattening is considered to be due to the increase in the secondary flow intensity with increase in Re_{bulk} . Figure 3 shows the calculated secondary flow distributions in a minimum unit flow cell of an infinite bundle with $P/D = 1.2$ for $Re_\tau = 400$ and 1,400, where the vortex center is shown also to shift to the narrower gap region in highly turbulent flows.

3.4. Influence of Pitch to Diameter Ratio on Turbulent Flow Fields

In comparison with the result for $P/D = 1.2$, differences in the axial velocity profile for $P/D = 1.1$ and 1.05 with $Re_\tau = 400$ and 600 extend between those at center region and gap region as shown in Fig. 4. It is caused by the increase in relative flow area of the center region (toward $\phi = 30^\circ$) and the decrease in gap region (toward $\phi = 0^\circ$) as P/D decreases. Figure 5 shows the wall shear stress variations for $P/D = 1.2, 1.1, \text{ and } 1.05$ for $Re_\tau = 400$. The wall shear stress distribution varies over wider range with the decrease in P/D .

With a decrease in P/D the distribution of secondary flow vorticity for $P/D = 1.1$ and 1.05 becomes steep and its peak

is higher. This results from the increase of turbulent anisotropy due to a deformation of flow area. For $P/D = 1.05$, in particular, the maximum of the contour can be seen near the wall at $\phi = 21^\circ$ and $y_t/y_{\text{rmax}} = 0.05$. Three components of the Reynolds normal stress become larger as P/D decreases. This could be explained by the increase in the turbulent production near the wall due to an increase in the wall surface to flow area ratio as P/D decreases. In general the secondary flow vorticity concentrates in the vicinity of the pin wall as P/D decreases, and the turbulence anisotropy is enhanced in the gap region of the tight lattice bundles. Also it has been shown that the present numerical method could provide better physical descriptions of the Reynolds stress including the behaviors of its azimuthal components in the gap region of a tight lattice bundle, which is difficult to obtain by such classical CFD approaches as solving the RANS equations.

4. CONCLUDING REMARKS

In summary, the DNS results are judged to lie within the error ranges of the experiment for the axial velocity profile and wall shear stress distribution, and within 20% in Reynolds stress profiles at the localized region. Rigorously speaking, the higher Re turbulent flow simulation ($Re_{\text{bulk}} \cong 24,000$) is not regarded as DNS but pseudo-DNS in

the sense that it employs somewhat larger computing meshes than required. However, agreement with experiment is considered satisfactory from engineering point of view. In general the DNS calculations of flows in an infinite array pin bundle are considered to be reliable in this work.

REFERENCES

- [1] Rapley, C.W., Gosman, A.D., 1986. The prediction of fully developed axial turbulent flow in rod bundles, *Nucl. Eng. Des.*, **97**, pp.313-325
- [2] Lee, K.B., Jang, H.C., 1997. A numerical prediction on the turbulent flow in closely spaced bare rod arrays by a nonlinear k- ϵ model, *Nucl. Eng. Des.*, **172**, pp.351-357
- [3] Baglietto, E. and Ninokata, H., 2004. CFD modeling of secondary flows in fuel rod bundles, N6P363, 6th Int. Top. Mtg on Nuclear Reactor Thermal Hydraulics, Operations and Safety (NUTHOS-6), Nara.
- [4] Zhang, Y., Street, R.L., and Koseff, J. R., 1994. A non-staggered grid, fractional step method for time-dependent incompressible Navier-Stokes equation in curvilinear coordinates", *J. Comput. Phys.*, **114**, pp.18-33
- [5] Trupp, A.C., and Azad, R.S., 1975. The structure of turbulent of flow in triangular array rod bundles, *Nucl. Eng. Des.*, **32**, pp.47-84

高速炉炉心稠密燃料集合体サブチャネル内直接乱流シミュレーション

プロジェクト責任者

二ノ方 寿 東京工業大学大学院原子核工学専攻

著者

二ノ方 寿^{*1}, 阿竹 規男^{*1}, Emilio Baglietto^{*1}, 三沢 丈治^{*2}, 叶野 琢磨^{*2}

*1 東京工業大学大学院

*2 日本原子力研究所

境界適合型座標系上で高速炉燃料集合体内乱流DNSを実施して、P/D（格子間隔対燃料ピン直径比）およびRe数への乱流特性依存性データを取得した。とくに、低Re乱流（ $Re_{\tau}=400$ ）条件下で稠密格子（ $P/D < 1.1$ ）における燃料ピン間狭隘ギャップでの局所的層流遷移の発現、および低Re $_{\tau}$ における各種統計量空間分布形状のRe依存性が高Re $_{\tau}$ （1,000~1,400）の領域では低下するなど、燃料格子配列内の実験的に取得が困難な乱流特性に関する知見が得られた。

高速炉炉心燃料のようにP/Dが小さい稠密格子燃料集合体内サブチャネル内の乱流は、燃料要素間隔が狭いために壁の影響を強く受け、非等方性が強い。そのため、等方性乱流を仮定したk-εモデルや、壁関数を用いたモデルでは説明できない現象が多い。一般的に燃料集合体内の乱流は、P/Dの減少およびRe数が低くなると燃料間隙部近傍でその非均質性が増すとともに、局所的な乱流-層流遷移領域を含み、流れそのものが不安定となることが予測される。本研究は、これらの予測をDNSによって数値的に確認し、実験的に取得困難な乱流データを設計および安全評価へ提供することを目的とする。

図1にDNSで計算された y^+ 方向の w^+ 分布を、燃料間隙部からの角度 $\phi = 0, 15, 30^\circ$ の各位置で、Reichardtによる壁関数と比較して示す。なお $\phi = 0$ は燃料ピン間のギャップ位置である。ちなみに乱流の非等方性を考慮しない場合、二次流れによるモメンタムの再配分が行われず、ギャップ位置から遠ざかるにつれ、軸方向流速 w^+ の y^+ 方向分布が壁近傍で急峻となり壁せん断応力が増加する。一方、非等方性を考慮すると、二次流れによって全体的に w^+ 分布が平坦化され、壁せん断応力分布のピークが $\phi \sim 20^\circ$ 近傍にシフトする。図2に $Re_{\tau}=400$ （ $Re_{bulk} \sim 6,000$ ）のときのDNSによる平均値で規格化した壁せん断応力分布 $\tau_w/\tau_{w,av}$ を、異なるP/Dについて比較して示す。このような比較的低Re数の領域では、同一のRe数に対し、格子配列が稠密になるほど（ $P/D \sim 1.05$ ） τ_w のピーク値が高くなる。P/D=1.2に対しRe数を増加させると、 $\tau_w/\tau_{w,av}$ のピークが下がり続け、あるRe数を境に形状が一定になることがDNS計算で示された。実際、 $Re_{\tau}=1,000, 1,400$ （ $Re_{bulk} \sim 16,000, 24,000$ ）で、 τ_w 分布は概ね同一形状となる。 $\phi \sim 25^\circ$ 近傍に位置するピーク値は平均値の105%で、 $Re_{\tau}=400$ の108%に比べて低下することが、二次流れ分布の変化から示された。これらのDNS結果は、ピーク位置（ $\phi \sim 25^\circ$ ）で、 τ_w 分布形状がRe数（23,760~56,000）に依存しないという従来の実験事実と合致する。同様にレイノルズ応力の分布など各種乱流統計量についても $Re_{\tau}=1,000 \sim 1,400$ の範囲でその分布に大きな変動がなく、P/D=1.2の場合 $Re_{\tau}=1,000$ の近傍で漸く完全乱流領域へ移行するものと判断される。

なお、集合体内乱流の詳細な乱流測定データが過去にいくつか報告されているが、P/D < 1.1または $Re < 20,000$ の条件下のデータの報告はない。これらのことより、実験に替わるDNS計算の有用性、実用性が本研究により示された。

キーワード：直接乱流シミュレーション，乱流非等方性，二次流れ，燃料集合体，サブチャネル

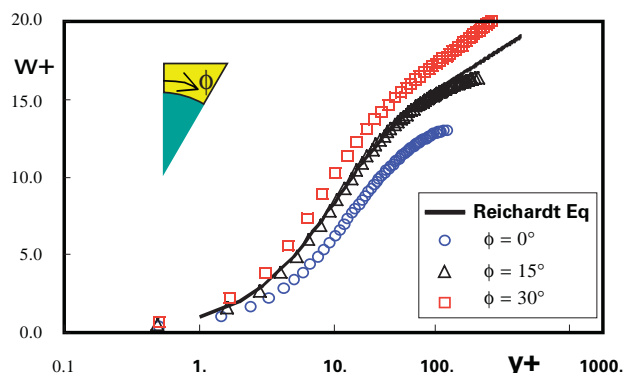


図1 DNSと壁関数による流速分布の比較（P/D=1.05; Re=9,500）

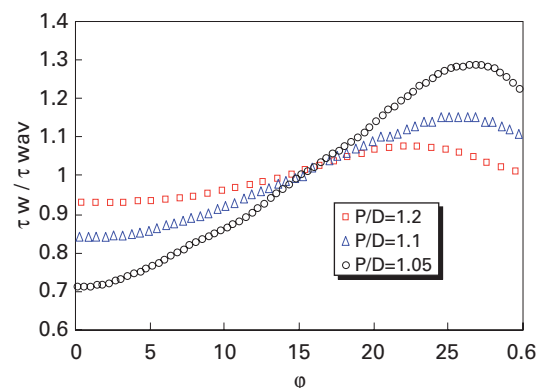


図2 壁せん断応力分布のP/D依存性（Re=6,000）